Structural, redox and catalytic chemistry of ceria based materials

G. Ranga Rao* and Braja Gopal Mishra
Department of Chemistry, Indian Institute of Technology Madras, Chennai 600036, India

Abstract
The article gives an overview on the ceria and ceria-based materials describing structural and redox properties. The affect of surface area, dopant and metal-ceria interactions on the reduction characteristics is examined by taking specific examples. The importance of ceria-based materials in heterogeneous catalysis, exhaust catalysis in particular, is highlighted.
Keywords: ceria, TPR, redox property, ceria-zirconia

1. Introduction

Ceria-based materials continue to be investigated for their structural and chemical properties [1,2], reduction behaviour and non-stoichiometry [3], oxygen storage capacity [4-6] and metal-ceria interactions [7,8]. These materials show promising applications in environmental catalysis [4, 6, 9-15], redox catalysis [1-8] and wet catalytic oxidation of organic pollutants [15, 16]. Single crystal ceria surfaces and thin films have also been employed to study model catalytic reactions [17,18]. The prominent role of ceria has been recognised in three-way catalysis, catalytic wet oxidation, water-gas-shift reaction, oxidation/combustion catalysis and solid oxide fuel cells [1,11, 10-19]. The structural features of ceria in combination with oxygen storage and release properties are crucial for various catalytic reactions. Ceria can be employed as an oxide carrier or a mixed oxide carrier with a transition metal oxide providing unique catalytic properties.. Ceria is also believed to help in preserving the catalyst surface area, pore size distribution and catalytic activity [1-7]. A number of CeO_2-based systems such as CeO_2-ZrO_2, CeO_2-Al_2O_3, $CuO/CeO_2/Al_2O_3$ CeO_2-SiO_2, CeO_2-La_2O_3, CeO_2-HfO_2, Pd/CeO_2 and Au/CeO_2 have been examined for their catalytic properties [1,2, 7-11]. Recently efforts have also been made to synthesize nanoparticles of ceria having better physicochemical properties for diverse applications [20]. The present article provides an overview of some structural and catalytic aspects of ceria-based mixed oxides and supported metal systems.

2. Structural features of CeO_2

The structural properties of CeO_2 have been investigated by several authors providing valuable information on redox properties and oxygen mobility in the ceria lattice [21-23]. Ceria is a pale yellow color solid due to $O^{2-} \leftarrow Ce^{4+}$ charge transfer and is known to crystallize in fluorite structure (CaF_2) with a space group of Fm3m. The unit cell of ceria is shown in figure 1. In the face centered cubic (FCC) structure of ceria, Ce^{4+} ions form a cubic close packing arrangement and all the tetrahedral sites are occupied by the oxide ions whereas the octahedral sites remain vacant. The unit cell of ceria can

* Corresponding author, Email-grrao@iitm.ac.in

be considered as a simple cube, in which the face center positions and corners are occupied by Ce^{4+} ions. The tetrahedral sites can be visualized by dividing the cube into eight smaller cubes. The body center positions of all the small cubes are occupied by oxide ions and the alternate corners are occupied by Ce^{4+} ions.

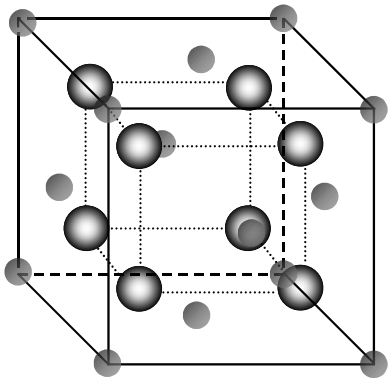

Figure 1. Fluorite structure of CeO_2.

Under reducing atmosphere, ceria is known to form nonstoichiometric oxides of general composition CeO_{2-x} where $0<x<0.5$. The extent of reduction of ceria and the formation of non-stoichiometric phases have been studied by using several techniques such as TPR, XRD and magnetic measurements [3-8, 21]. The fluorite structure of ceria is retained up to 900 K under reducing atmosphere. However, the lattice parameter is found to increase with reduction temperature indicating an expansion in the FCC lattice [21, 24]. An increase of 1.8% in the lattice parameter with respect to stoichiometric ceria after the reduction treatment at 873 K has been reported [21]. This conclusion has also been arrived at from the thermal expansion and molar volume measurements [22,23]. The increase in the lattice parameter is attributed to the reduction of Ce^{4+} ions to Ce^{3+}. The radius of Ce^{3+} is larger than the radius of Ce^{4+} resulting in the lattice expansion. The non-stoichiometric phases formed during the reduction process can be easily oxidized to the pure CeO_2 phase upon exposure to air or under mild oxidizing conditions. However, the reversibility of this process is decreased when ceria is reduced at higher temperatures. When ceria is reduced at 1070-1170 K, a cubic Ce_2O_3 phase has been detected K [21]. The cubic Ce_2O_3 phase reoxidizes slowly in air compared to the expanded ceria phases. Reduction of ceria at temperatures greater than 1273 K leads to the formation of hexagonal Ce_2O_3 phase. This phase is stable at room temperature and possesses identical structure as that of La_2O_3. The ability of the cerium ion to switch between the Ce^{4+} and Ce^{3+} oxidation states depending on the ambient oxygen partial pressure is represented as:

$$CeO_2 \equiv CeO_{2-x} + x/2\ O_2 \qquad (1)$$

The amount of oxygen released in the forward reaction and the oxygen consumed in the reverse reaction is generally referred as the oxygen storage capacity (OSC) of ceria material [1-3]. The labile oxygen and possible large deviations from its stoichiometry are essentially the reasons for use of CeO_2 in three-way catalysts (TWC) [2, 6].

3. Ceria in Three Way Catalyst (TWC)

The most important application of ceria-based materials is exhaust catalysis which has been reviewed extensively [2,6,25,26]. The three-way catalysts are designed to simultaneously convert automobile exhaust pollutants (uncombusted hydrocarbons (HC), carbon monoxide (CO) and nitrogen oxides (NO_x)) to environmentally acceptable products such as carbon dioxide, water and nitrogen. The TWC

formulation contains Pt/Rh, Pt/Pd/Rh, Pd/Rh and Pd-only metal catalysts dispersed either on the surface of alumina pallets or on an alumina washcoat anchored to a monolithic substrate made of cordierite ($2MgO.2Al_2O_3.5SiO_2$) or a metal [2,6]. High surface area γ-alumina is used as support because of its higher thermal stability under hydrothermal conditions [6]. The thermal stability and surface area of γ-alumina has been further improved by adding oxides of Ce, Ba, La and Zr as stabilizing agents [2]. Among the precious metal combination, the Rh based bi- or tri-metallic catalysts show considerable activity for the reduction of NO_x compared to Pt and Pd catalysts [2, 25]. In addition, ceria and ceria-based mixed oxides such as CeO_2-ZrO_2 are used as oxygen storage promoters in TWC. The working conditions of TWCs are severe exposing them to unpredictable variations in temperature, pressure and reactant concentrations. An optimum performance of the TWC is possible if the stoichiometric air-fuel ratio (A/F) is maintained at 14.6 as shown in Fig.2.

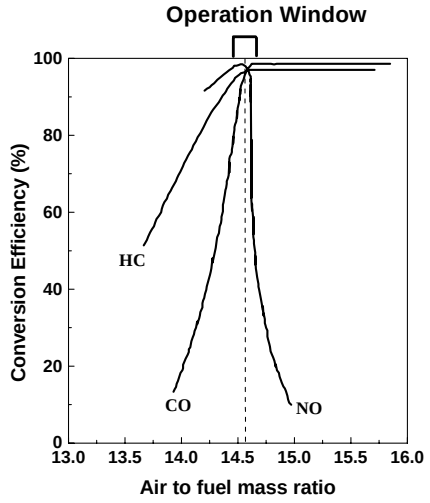

Figure 2. Effect of air to fuel ratio on the conversion efficiency of three-way catalyst.

If the air-fuel ratio is close to the stoichiometric value of 14.6, the catalyst converts all the pollutants to CO_2, H_2O and N_2 gases with high efficiency. Deviation from the stoichiometric value affects the performance of the three-way catalyst resulting in the incomplete conversion of the pollutants. Under fuel lean period the conversion of NO is affected whereas under fuel rich condition the oxidation of CO and hydrocarbons remains incomplete. The role of ceria and ceria based materials in TWC is to widen the A/F window and help maintaining the conversion efficiency of the catalyst. Ceria has the ability to store excess oxygen under fuel lean period and release it under fuel rich conditions for the oxidation of CO and hydrocarbons. This happens due to its ability to switch between Ce^{4+} and Ce^{3+} oxidation states depending on the oxygen partial pressure in the exhaust gas composition. Ceria can undergo a number of reactions by exchanging oxygen with gas molecules in the exhaust environment.

Under lean condtions

$Ce_2O_3 + 0.5\ O_2 \rightleftharpoons 2CeO_2$

$Ce_2O_3 + NO \rightleftharpoons 2CeO_2 + 0.5\ N_2$

$Ce_2O_3 + H_2O \rightleftharpoons 2CeO_2 + H_2$

Under rich conditions

$2CeO_2 + H_2 \rightarrow Ce_2O_3 + H_2O$

$2CeO_2 + CO \rightarrow Ce_2O_3 + CO_2$

In addition, ceria also helps in maintaining the dispersion of the noble metals and provides thermal stability to the γ-alumina phase. It also promotes water gas shift reaction ($CO + H_2O \rightarrow H_2 + CO_2$) during the transient oscillations in the exhaust, thus enhancing the CO oxidation [1,2,6].

Ceria-based transition metal binary oxides such as CeO_2-CuO have been found to be good catalysts for CO oxidation at very low light off temperatures [9, 10]. It is proposed that the reaction, $CO_{ad} + O_{lattice} \rightarrow CO_2$ (g), occurs between CO adsorbed on noble metal and the oxygen derived form the ceria lattice at the noble metal and ceria interface.

4. Redox property of ceria

The mobility of surface oxygen species in ceria is found to be higher compared the conventional oxides such as SiO_2, Al_2O_3, MgO and ZrO_2 [28]. These mobile surface oxygen species can be removed easily under reduction atmosphere leading to the formation of non-stoichiometric ceria, CeO_{2-x} ($0 \leq x \leq 0.5$) [21-23]. The Ce^{3+} ions form the main defect centers and the charge imbalance is neutralized by the formation of oxygen ion (O^{2-}) vacancies [3-5]. Ceria retains its fluorite structure when reduced at temperatures below 900 K. The reduced form of ceria can be completely oxidized when exposed to air at room temperature. This easy availability of lattice oxygen and retention of the structural feature has been exploited in several cases for catalytic reactions involving oxidative process [1,2,6,11]. The redox property of ceria has been studied using several experimental methods. However, temperature programmed reduction (TPR) is unique to study the temperature dependence reduction behavior of ceria based materials [3]. The reduction of ceria takes place essentially in two temperature regions (Fgure 3). The first region is 573-873 with T_{max} around 790 K and the second region is 973-1273 K with T_{max} around 1100 K. These two reduction regions are characteristics of ceria and are attributed to the surface and bulk reduction respectively [2,3,29]. The higher mobility of the surface oxygen ions helps in the removal of lattice oxygen during reduction process. The coordinately unsaturated surface capping oxygen ions can be easily removed in the low temperature region. However, bulk oxygen requires to be transported to the surface before their reduction. Consequently, the bulk reduction takes place at higher temperature compared to the surface reduction.

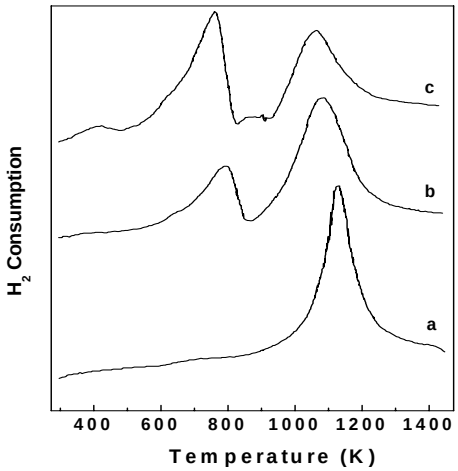

Figure 3. TPR profiles of CeO_2 samples having different surface areas, (a) 1.5 m^2/g, (b) 30 m^2/g and (c) 130 m^2/g.

Another important aspect to be noticed from figure 3 is that the hydrogen consumption in the low temperature region increases with the surface area of the ceria sample. A linear correlation has been observed between the surface area and the hydrogen consumption at the low temperature region [21]. The presence of a variety of surface capping oxygen ions can be expected in a small crystallite of ceria. A small crystallite surface may contain O^{2-} ions at different positions with different coordination numbers. For example, the oxide surfaces can have imperfections such as steps, kinks, and corners

projecting O^{2-} ions of different coordination number. The variety and population of such surface O^{2-} ions may increase with surface area. Based on the CeO_2 TPR and the results obtained from other techniques [21,30,31], a model has been proposed for ceria reduction [32]. The model consists of four steps (i) dissociation of chemisorbed hydrogen to form hydroxyl group, (ii) formation of anionic vacancies and reduction of neighboring Ce^{4+} ions, (iii) desorption of water by recombination of hydrogen and hydroxyl groups and (iv) diffusion of surface anionic vacancies into the bulk material. The kinetic model is shown schematically below in figure 4.

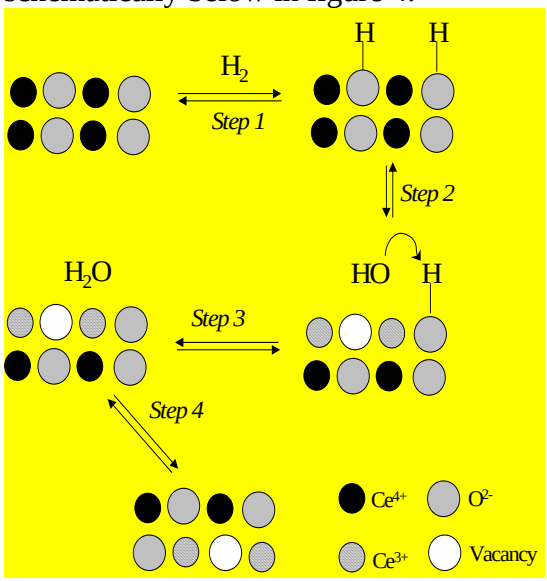

Figure 4. Ceria reduction mechanism [32].

The initial reduction process is very sensitive to the surface area of the ceria material (fig.3). The bulk reduction begins only after the complete reduction of the surface sites. The surface reduction of ceria through the formation of hydroxyl group has been studied by FT-IR spectroscopy [31]. Several types of hydroxyl groups differing in the coordination environment have been observed on the surface of ceria, the intensity of which depends on the procedure of preparation of these materials. The intensity of these OH stretching bands increases with increase in reduction temperature up to 673 K. At higher temperature these bands disappear due to the desorption of water leading to the formation of anion vacancy at the surface.

While using ceria based materials in catalytic processes such as three-way catalysis, the main concern is the thermal stability of the ceria component at higher temperatures. Ceria promoted three-way catalyst is often exposed to temperatures greater than 1200 K under the operating conditions. At such high temperatures, the oxygen storage capacity of ceria strongly decreases upon thermal aging due to the growth of ceria crystallite size loosing the active surface area and /or formation of $CeAlO_3$ phases [33]. The growth of ceria crystallite and the thermal sintering process can be considered as due to the mass transport at an atomic scale caused by a concentration gradient set at higher temperature. The sintering process of ceria has been explained through six elementary steps, oxygen adsorption, oxygen vacancy creation and diffusion, oxygen desorption, cerium vacancy diffusion or vacancy annihilation [34]. Improvement of the thermal properties of ceria and retention of active surface area at high temperature is thus necessary to exploit the redox property of ceria for various applications especially in TWC. Incorporation of aliovalent cations into the lattice of ceria improves its thermal stability besides affecting the physical properties of ceria such as density, ionic conductivity and lattice parameters [33]. The thermal

stability and redox behavior of ceria can be improved by incorporation of zirconia into ceria lattice [2-8]. Ceria is known to form a substitutional type solid solution with zirconia [5, 35]. The ceria-zirconia solid solutions show better oxygen storage capacity and reduction behavior compared to pure ceria and potential substitutes for ceria in TWC applications [2,3,36]. Ceria-zirconia solid solution exists in three different phases namely monoclinic, tetragonal and cubic. The cubic and monoclinic phases are thermally stable below 1300 K, where as the tetragonal phase is a metastable phase and can be prepared by high temperature ceramic method in the composition range of 10-50 mol% of ceria [7, 35]. Above 50 mol% of ceria, the cubic phase is formed. The kinetics of the redox process is favored in the cubic phase compared to the tetragonal and monoclinic phase [5]. There is dramatic change in the TPR profile of ceria upon the incorporation of zirconia into the ceria lattice. Figure 5 shows the TPR profiles of high surface area CeO_2-ZrO_2 solid solutions in comparison with the TPR profile of CeO_2.

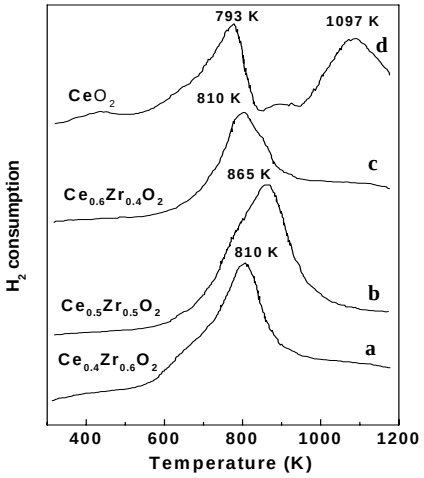

Figure 5. TPR profiles of CeO_2-ZrO_2 solid solutions and CeO_2.

The oxide solid solutions undergo reduction in the region between 500 K and 950 K with different T_{max} values. Two important observations can be made from figure 5. One is that the solid solutions undergo maximum reduction at temperatures close to the surface reduction of pure ceria and the other is the surface and bulk reduction signatures, observed for pure ceria, are merged together for the solid solutions. This suggests that the entire ceria component present in the solid solution is undergoing reduction in a single step. The change in reduction features has been explained in terms of facile migration of oxygen ions in the CeO_2-ZrO_2 lattice. The structural factor plays an important role in the reduction behavior of these oxide solid solutions and has been studied in details for samples prepared by high temperature solid state reaction [5]. The solid solution contains predominantly tetragonal phase for 10-50 mol% ceria content, whereas at higher ceria content the formation of cubic phase is favored. The oxygen diffusion in the defective fluorite structure of ceria has been explained by a vacancy mechanism [1,3]. A smaller cell volume requires less energy for the hopping of oxygen ions with in the lattice and favors the reduction process. The oxygen mobility in the lattice depends on the effective radius of the cation. The oxygen anions are in a tetrahedral coordination in the fluorite structure and their migration to the nearby tetrahedral position occurs through the channel formed by nearby cations. The dependence of the channel radius on the ceria content is shown in figure 6.

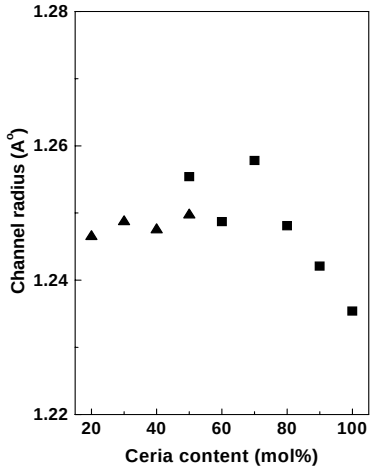

Figure 6. Channel radius for oxygen migration in the tetragonal (▲) and cubic (■) structures [5].

For the tetragonal structure the channel radius almost remains constant with ceria content whereas for the cubic phase the channel radius is found to decrease with increase in ceria content (except 70 mol% ceria). The optimum channel radius is found to be in the ceria content of 50-60 mol%. Consequently, for these compositions the oxygen mobility will be higher favoring the process of reduction. Figure 6, clearly suggests that in the cubic samples the process of reduction is facilitated by the substitution of Ce^{4+} with Zr^{4+}.

Ceria based mixed oxides of V, Mn, Ni, Co and Cu have also been studied form the point of their redox property and catalysis. Several catalytic transformation such as steam reforming [1,37], oxidative adsorption of NO [38], oxidation of CO [9], total oxidation of hydrocarbon [39] are promoted by the presence of transition metal ions in ceria lattice. The interaction between the transition metal ions and ceria lattice is crucial for the catalytic activity of the composite oxides. For example, in the case of Cu-Ce-O composite oxides a synergistic model has been invoked to explain the enhanced catalytic activity for CO oxidation and methane combustion [9,40]. The Cu-Ce-O composite catalyst shows remarkable catalytic activity for CO oxidation with light off temperature as low as 343 K [9,10]. The activity of the material has been attributed to the direct participation of the Cu^{2+}/Cu^{+} couple stabilized by chemical interaction with ceria. The interaction of CuO particles with ceria has been studied by thermal, surface and bulk techniques. These studies have shown the presence of variety of copper species with different coordination and dispersion on the surface of ceria [9,40,41]. The extent CuO dispersion and the interaction with ceria also depend upon the preparative method of the composite oxide. For example a CuO(20%)-CeO_2 oxide prepared by combustion method shows different low temperature reduction features compared to the same material prepared by conventional precipitation method (figure 7). The sample prepared by the precipitation method shows a broad reduction feature at low temperature region with T_{max} at 240^{o}C corresponding to the reduction of supported CuO particles (fig 7a). However, the reduction of the composite catalyst prepared by combustion method occurs at much lower temperature with two TPR peaks at 145 and 170^{o}C. In addition to that, the high temperature peak corresponding to the bulk reduction of ceria is shifted by about 40^{o}C to lower temperature. This is due to the fact that the dispersion of CuO particles is not the same in both cases and that there are two types of copper oxide species existing in the combustion synthesized sample [41]. These CuO phases contain highly dispersed copper oxide species and bulk

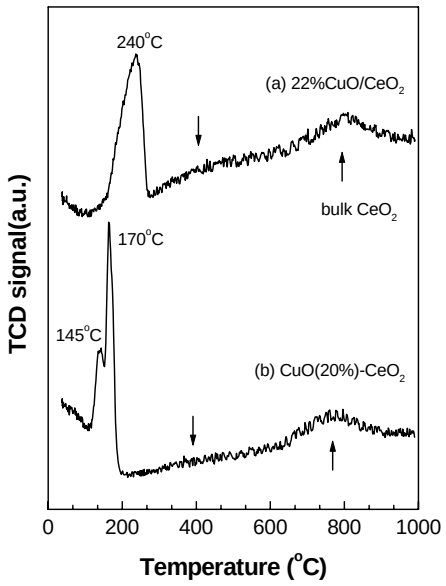

Figure 7. TPR profiles for (a) 22%CuO/CeO_2 prepared by precipitation and (b) combustion synthesized CuO (20%)-CeO_2 composite oxide.

like CuO particles present on the ceria surface. Moreover, the shift in the reduction peaks to low temperature for both CuO and ceria indicate a strong interaction between the oxide components mutually influencing the redox property of each other. This type of mutually promoting synergistic effect between CeO_2 and CuO is believed to be essential for higher catalytic activity of CuO/CeO_2 catalysts for CO oxidation [9].

5. Metal-ceria interactions

Supported metals are used in large scale in heterogeneous catalysis. The role of the support is to disperse the metal particles and maintain them from sintering. The supports widely used are SiO_2, Al_2O_3, TiO_2, Nb_2O_5, CeO_2 and ZrO_2. In addition to the dispersion of the metallic components the support can influence the electronic and catalytic properties of the supported metal particles by electron transfer or chemical bond formation. Metal support interactions have been extensively studied by using chemisorption techniques after the discovery of the strong metal support interaction (SMSI) effect by Tauster et al [42]. The occurrence of SMSI has been well established for reducible support such as TiO_2 and Nb_2O_5 using chemisorption of hydrogen and carbon monoxide as probe molecules. At high reduction temperature, the partially reduced support covers the surface of the metal particles, thereby blocking the sites for H_2 and CO chemisorption and catalysis [43]. The SMSI effect has been observed on (i) reducible supports, (ii) induced by high temperature reduction treatment (> 800 K), (iii) accompanied by significant changes in chemisorptive and catalytic properties of the supported metal and (iv) is reversible. The reducible nature of ceria and ceria-based composite oxides prompted some investigations to examine the SMSI phenomenon in these materials [1,44]. Ceria supported Pt [45,46], Pd [45,47], Rh [45, 48], Ni [49] and Ru [45,50] metals have been investigated for metal-support interactions and catalytic applications. Despite large number of investigations, no clear picture seems to have emerged on metal-ceria interactions. In some cases the metal ceria interaction has been ascribed to classical SMSI where as in other cases alternative explanations have been proposed [1,44]. For example for Pt supported on TiO_2 and CeO_2, though a decrease in hydrogenolysis activity has been observed for both the catalysts after high temperature reduction at 773 K, the surface morphology of the Pt/CeO_2 catalyst is little affected unlike the Pt/TiO_2 catalyst. HRTEM study of

Pt/TiO_2 reveals that after HTR, the supported Pt particles were covered with an overlayer of titania support. However, no such overlayer has been observed for Pt supported on ceria and no difference in the Pt structure was observed in the HTR state or after reoxidation followed by low temperature reduction [46]. The formation of Pt-Ce alloy has been proposed, in an earlier study, to account for the difference in the chemisorption and catalytic behaviour of Pt/CeO_2 and Pt/TiO_2 catalysts [51]. Similarly, for Pd/Ceria systems no considerable decrease in the H_2 and CO chemisorption or CO methanation have been observed after high temperature reduction [52]. Encapsulation of Pd by reduced ceria occurs at reduction temperature higher than 973 K. The interaction of Pd with ceria has been studied by using HRTEM and XRD techniques [47]. Three prominent changes has been observed after reduction at 973 K, (i) epitaxial growth of small Pd particles on CeO_2, (ii) decoration of large particles of Pd with ordered CeO_2 overlayer and (iii) Expansion of the lattice parameters of Pd. For Rh/CeO_2 system the hydrogen chemisorption is not suppressed by high temperature reduction [48]. Hydrogen spillover from the Rh metal surface to the ceria support has been detected for this system resulting in complete reduction of ceria surface [53]. The interaction between the Rh metal and ceria has been studied by HRTEM [54]. No evidence of metal decoration has been observed for Rh/CeO_2 up to reduction temperature 773 K. The activity of the catalyst also does not change appreciably with the reduction temperature. Sanchez and Gasquez have proposed a general model on the basis of structural considerations to account for the difference in the metal support interaction in M/TiO_2 and M/CeO_2 [55]. Titania has a casserite (SnO_2) like structure whereas ceria crystallizes in fluorite structure. For M/TiO_2 system, due to the relatively open structure of the cationic sublattice of titania, the migration of the surface metal to the bulk of the titania takes place during high temperature reduction. Consequently, the metals are buried inside the bulk of the support resulting in a loss of the adsorptive and catalytic properties. For fluorite structured ceria, however, the cationic sublattice provide an activation barrier for the migration of the metal atoms to the bulk. The authors provided an alternative explanation for the ceria supported metal system. They propose the anchoring of the metal crystallite on the surface oxygen vacancies of ceria created by high temperature reduction [55]. This model explains the absence of any drastic change in adsorption and catalytic properties of M/CeO_2 materials along with the resistance of the metal particles from thermal sintering.

The M/CeO_2 systems have been extensively used as catalysts for several industrially and environmentally important chemical reactions [1,2,9,11,]. Particular attention has been given to the noble metals such as Pt, Pd and Rh because of their use in three way catalysts. Numerous studies on metal supported ceria, however, clearly point to the active role of ceria in catalytic processes. Ceria influences the catalytic property of the supported metal by metal-support interaction. The oxygen storage capacity, Ce^{4+}/Ce^{3+} redox couple and the defect sites such as anionic vacancies at the metal-ceria interface can directly contribute to the catalytic

activity of the ceria-supported materials. In certain cases mutual promoting effect between ceria and metal component has been found to be the cause for higher catalytic activity [3,5-7,56]. For example, in $Pd/CeO_{2-x}/Al_2O_3$ system the synergistic effect between the supported Pd metal and CeO_2 has been observed during methane oxidation reaction [56]. The ^{18}O tracer study clearly indicates the reversible migration of oxygen species between the Pd metal and the nonstoichiometric ceria lattice. In addition to the metal support interaction, the supported metal can also influence the phyicochemical properties of ceria support such as the oxygen storage capacity and reducibility [3-8]. The presence of a small amount of Rh has been found to modify the low temperature reducibility of ceria [3,4,35]. Figure 8 shows the TPR profiles of CeO_2 samples of different surface area with 0.5% Rh metal loading. The intensity of the low temperature reduction feature is found to increase with increase in surface area of the ceria support. However, the most important feature in fig. 8 is the decrease in the reduction temperature of surface oxygen species of ceria from 790 K to 400 K, which clearly indicates that the presence of Rh facilitates the surface reduction of ceria. This has been explained on the basis of spillover of hydrogen from Rh metal to the ceria surface resulting in facile reduction of the surface oxygen species [4]. Incorporation of zirconia into ceria lattice in the presence of Rh further facilitates the surface and bulk reduction process of ceria [4,5,35]. In the presence of Rh the ceria component in all the solid solutions is completely reduced below 500 K (fig. 9) while the bulk of

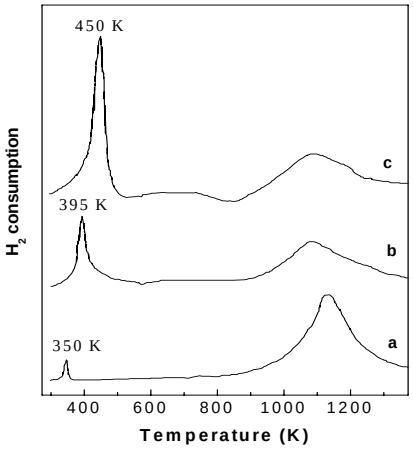

Figure 8. TPR profiles of calcined 0.5% Rh/CeO_2 with CeO_2 surface areas: (a) 1.5 m^2/g, (b) 30 m^2/g and (c) 130 m^2/g.

pure ceria required higher temperatures up to 1100 K for complete reduction (fig.8).

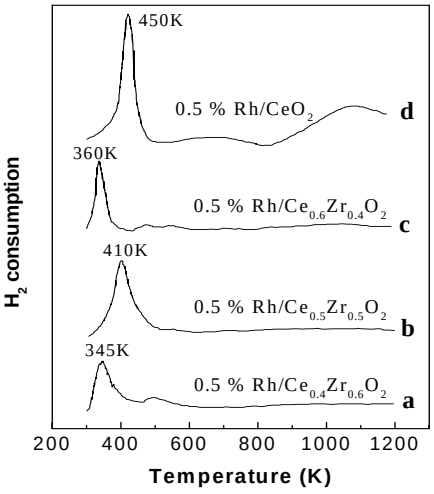

Figure 9. TPR profiles of calcined 0.5 % Rh/CeO_2-ZrO_2 samples with surface area; (**a**) 75 m^2/g, (**b**) 98 m^2/g, (**c**) 60 m^2/g and (d) 130 m^2/g.

The oxygen storage capacity (OSC) of ceria is also modified significantly in presence of Rh metal on its surface and by incorporation of zirconia into ceria lattice (Table 1). The formation of

Table 1. Hydrogen consumption and oxygen uptake of Rh/CeO_2 and Rh/CeO_2-ZrO_2 [5].

CeO_2 content (mol%)	H_2 consumption[a] (mlg^{-1})	Temperature (K)	O_2 uptake		Activation energy (kcal mol^{-1})
			mlg^{-1}	Mol O_2/mol Ce (x100)	
100[b]	26.2	700	4.5	3.2	3.40 ± 0.15
100[c]	8.6	700	3.9	2.7	
100[d]	1.4	700	0.16	0.11	
50[e]	18.3	700	9.4	11.3	1.73 ± 0.08
		600	9.0	10.9	
		550	8.5	10.3	

[a] Hydrogen consumed in TPR proceeding the OSC measurement
[b] Surface area 130 m^2/g
[c] Surface area 30 m^2/g
[d] Surface area 1.5 m^2/g
[e] Cubic CeO_2-ZrO_2 sample

structural defects and the facile reduction of the surface oxygen are the major factors responsible for the increase in the oxygen storage capacity. The Rh/CeO_2 samples show a significant increase of oxygen uptake on increasing the surface area. This clearly indicates that the surface reduction process contributes to the oxygen storage capacity of ceria since surface reduction is strongly favored on high surface area ceria. The Rh loaded CeO_2-ZrO_2 sample takes up significantly more oxygen than Rh/CeO_2 sample. Comparing the mole of O_2 uptake per mole of Ce, it is evident that the $Ce^{3+} \leftrightarrow Ce^{4+}$ redox cycle is more efficient in case of CeO_2-ZrO_2 compared to the pure ceria. The activation energy of oxygen uptake is significantly less in case of the ceria-zirconia solid solutions. As discussed in the previous section, the insertion of zirconia into ceria lattice induces formation of defect sites. Consequently, the oxygen mobility in the bulk is strongly enhanced resulting in the high OSC observed for this sample [4-7,35]. Rh loaded ceria and ceria-zirconia solid solutions have been found to show good catalytic activity for NO reduction by CO [4,5,7,8,35].

6. Conclusions

Ceria exhibits unique redox properties which can be attributed to the retention of the fluorite structure. Surface oxygen ions are easily removed during reduction compared to the bulk oxygen ions. Doping with Zr^{4+} ions enhances the oxygen mobility in ceria and the materials can be reduced/oxidised at lower temperatures. Oxygen storage capacity increases considerably in the Zr-doped ceria samples. In addition to the redox nature, metal-ceria interactions are crucial for oxygen exchange and catalytic properties. The method of preparation matters in the dispersion/incorporation of transition metal oxides in ceria. CuO dispersion on ceria by combustion synthesis shows the presence of variety of copper oxide species.

Acknowledgement: The authors would like to thank Professors M. Graziani and

J. Kašpar for their kind help and support in carrying out part of this work.

References

1. A. Troveralli, Catal. Rev. Sci. Eng., 38 (1996) 439.
2. J. Kašpar, M.Graziani, and P.Fornasiero, "Handbook on the Physics and Chemistry of Rare Earths", K.A. Gschneidner, Jr. and L.Eyring, eds, Elsevier Science B.V., Amsterdam, vol. 29, Ch.184, (2000) pp. 159-267.
3. G. Ranga Rao, Bull. Mater. Sci. 22 (1999) 89.
4. G. Ranga Rao, J. Kašpar, S. Meriani, R.D. Monte and M. Graziani, Catal. Lett. 24 (1994) 107.
5. P. Fornasiero, R. Di Monte, G. Ranga Rao, J. Kašpar, S. Meriani, A. Trovarelli and M. Graziani J. Catal., 151 (1995) 168.
6. J. Kašpar, P. Fornasiero and N. Hickey, Catal. Today 77 (2003) 419.
7. G. Ranga Rao, P. Fornasiero, R. Di Monte, J. Kašpar, G. Vlaic, G. Balducci, S. Meriani, G. Gubitosa, A. Cremona and M. Graziani, J. Catal. 162 (1996) 1.
8. P. Fornasiero, G. Ranga Rao, J. Kašpar, F.L. Erario and M. Graziani, J. Catal. 175 (1998) 269.
9. W. Liu, and M. Flytzani-Stephanopoulos, Chem. Eng. J. 64 (1996) 283.
10. Y. Li., Q. Fu and M. Flytzani-Stephanopoulos, Appl. Catal. B: Environ. 27 (2000) 179.
11. A. Trovarelli, C. de Leitenburg, M. Boaro and G. Dolcetti Catal. Today, 50 (1999) 353.
12. X. Wang and R. J. Gorte, Appl. Catal. A: Gen. 247 (2003) 157.
13. J. A. Montoya, E. Romero-Pascual, C. Gimon, P. Del Angel and A. Monzón, Catal. Today 63 (2000) 71.
14. N. Hickey, P. Fornasiero, J. Kašpar, M. Graziani, G. Martra, S. Coluccia, S. Biella, L. Prati and M. Rossi, J. Catal. 209 (2002) 271.
15. Imamura, S., Y. Okumura, T. Nishio, K. Utani and Y. Matsumura, Ind. Eng. Chem. Res. 37 (1998) 1136.
16. G. Neri, A. Pistone, C. Milone and S. Galvagno, Appl. Catal. B: Environ. 38 (2002) 321-329.
17. M. A. Henderson, C. L. Perkins, M. H. Engelhard, S. Thevuthasan and C. H. F. Peden, Surf. Sci. 526 (2003) 1.
18. Z. Xu, Z. Qi and A. Kaufman, J. Power Sources 115 (2003) 40.
19. S. Zha, J. Cheng, Q. Fu and G. Meng, Mater. Chem. Phys. 77 (2003) 594.
20. N. Izu, W. Shin and N. Murayama, Sensors and Actuators B: Chem 93 (2003) 449.
21. V. Perrichon, A. Laachir, G. Bergeret, R. Frety and L. Tournayan, J. Chem. Soc. Faraday Trans. 90 (1994) 773.
22. M. Ricken, J. Nolting and I. Riess, J. Solid State Chem. 54 (1984) 89.
23. R. Korner, M. Ricken, J. Nolting and I.24.Riess, J. Solid State. Chem. 78 (1989) 136.
25. S. P. Ray, A. S. Nowick and D.E. Cox, J. Solid State Chem. 15 (1975) 344.
26. R. J. Farrauto and R.M. Heck, Catal. Today 51 (1999) 351.
27. M. Shelef and R.W. McCabe, Catal. Today 62 (2000) 35.
28. C. Hardacre, R.M. Ormerod and R.M. Lambert, J. Phys. Chem. 98 (1994) 10901.
29. D. Martin and D. Duprez, J. Phys. Chem. 100 (1996) 9429.
30. H.C. Yao and Y.F.Y. Yao, J. Catal. 86 (1984) 254.
31. A. Laachir, V. Perrichon, A. Badri, J. Lamotte, E. Catherine, J.C. Lavalley,

J.E. Fallah, L. Hilaire, F. Normand, E. Quemere, G.N. Sauvion and O. Touret, J. Chem. Soc. Faraday Trans. 87 (1991) 1601.
32. C. Binet, A. Badri and J.-C. Lavalley, J. Phys. Chem. 98 (1994) 6392.
33. J.E. Fallah, S. Boujana, H. Dexpert, A. Kiennemann, J. Majerus, O. Touret, F. Villain and F.L. Normand, J. Phys. Chem. 98 (1994) 5522.
34. J.Z. Shyu, W.H. Weber and H.S. Gandhi, J. Phys. Chem. 92 (1988) 73.
35. P. Maestro and D. Huguenin, J. Alloys comp. 225 (1995) 520.
36. G. Ranga Rao, P. Fornasiero, J. Kaspar, S. Meriani, R.D. Monte and M. Graziani, Stud. Surf. Sci. Catal. 96 (1995) 631.
37. A. Martinez-Arias, M. Fernandez-Garcia, A. Iglesias-Juez, A.B. Hungria, J.A. Anderson, J.C. Conesa and J. Soria, Appl. Catal. B: Environ. 38 (2002) 151.
38. D. Srinivas, C.V.V. Satyanarayana, H.S. Potdar and P. Ratnasamy, Appl. Catal. A: Gen. 246 (2003) 323.
39. M. Machida, M. Uto, M. Kurogi and T. Kijima, J. Mater. Chem. 11 (2001) 900.
40. F. Zamar, A. Trovarelli, C. de Litenburg and G. Dolcetti, J. Chem. Soc. Chem. Commun. (1995) 965.
41. P. Bera, S.T. Aruna, K.C. Patil, M.S. Hegde, J. Catal. 186 (1999) 36.
42. G. Ranga Rao, H. R. Sahu and B.G. Mishra, Colloids Surf. A: Physicochem. Eng. Aspects 220 (2003) 261.
43. S.J. Tauster, S.C. Fung and R.L. Garten, J. Am. Chem. Soc. 100 (1978) 170.
44. D.E. Resasco and G.L. Haller, J. Catal. 82 (1983) 279.
45. S. Bernal, J.J. Calvino, M.A. Cauqui, J.M. Gatica, C. Larese, J.A. Perez Omil, J.M. Pintado, Catal. Today 50 (1999) 175.
46. C. de Leitenburg, A. Trovarelli and J. Kašpar, J. Catal. 166 (1997) 68.
47. A.K. Datye, S.K. Kalakkad, M.H. Yao and D.J. Smith, J. Catal. 155 (1995) 148.
48. T. Bunluesin, R.J. Gorte and G.W. Graham, Appl. Catal. B: Environ. 14 (1997) 105.
49. S. Imamura, T. Yamashita, R. Hamada, Y. Saito, Y. Nakao, N. Tsuda and C. Kaito, J. Mol. Catal. A: Chem. 129 (1998) 249.
50. V.D. Belyaev, T.I. Politova, O.A. Marina, V.A. Sobyanin, Appl. Catal. A: Gen. 133 (1995) 47.
51. Y. Niwa and K. Aika, J. Catal. 162 (1996) 138.
52. P. Meriaudeau, J.F. Dutel, M. Dufaux and C. Naccache, Stud. Surf. Sci. Catal. 11 (1992) 95.
53. M.D. Mitchel and M.A. Vannice, Ind. Eng. Chem. Fundam. 23 (1984) 88.
54. S. Bernal, J.J. Calvino, G.A. Cifredo, J.M. rodriguez-Izquierdo, V. Perrichon and A. Laachir, J. Catal. 137 (1992) 1.
55. S. Bernal, J.J. Calvino, M.A. Cauqui, G.A. Cifredo, A. Jabacho and J.M. Rodriguez-Izquierdo, Appl. Catal. A: Gen. 99 (1993) 1.
56. M.G. Sanchez and J.L.Gazquez, J. Catal. 104 (1997) 120.
57. M. Haneda, T. Mizushima and N. Kakuta, J. Phys. Chem. B 102 (1998) 6579.